Available online at www.sciencedirect.com
SCIENCE DIRECT®
International Journal of Mass Spectrometry 240 (2005) 233–248
International Journal of Mass Spectrometry
www.elsevier.com/locate/ijms

Sequential bond energies of water to sodium glycine cation

S.J. Ye, R.M. Moision, P.B. Armentrout*

Department of Chemistry, University of Utah, Salt Lake City, UT 84112, USA

Received 17 July 2004; accepted 27 September 2004
Available online 24 November 2004

Abstract

Absolute bond dissociation energies of water to sodium glycine cations and glycine to hydrated sodium cations are determined experimentally by competitive collision-induced dissociation (CID) of $Na^+Gly(H_2O)_x$, $x = 1$–4, with xenon in a guided ion beam tandem mass spectrometer. The cross sections for CID are analyzed to account for unimolecular decay rates, internal energy of reactant ions, multiple ion–molecule collisions, and competition between reaction channels. Experimental results show that the binding energies of water and glycine to the complexes decrease monotonically with increasing number of water molecules. Ab initio calculations at four different levels show good agreement with the experimental bond energies of water to $Na^+Gly(H_2O)_x$, $x = 0$–3, and glycine to $Na^+(H_2O)$, whereas the bond energies of glycine to $Na^+(H_2O)_x$, $x = 2$–4, are systematically higher than the experimental values. These discrepancies may provide some evidence that these $Na^+Gly(H_2O)_x$ complexes are trapped in excited state conformers. Both experimental and theoretical results indicate that the sodiated glycine complexes are in their nonzwitterionic forms when solvated by up to four water molecules. The primary binding site for Na^+ changes from chelation at the amino nitrogen and carbonyl oxygen of glycine for $x = 0$ and 1 to binding at the C terminus of glycine for $x = 2$–4. The present characterization of the structures upon sequential hydration indicates that the stability of the zwitterionic form of amino acids in solution is a consequence of being able to solvate all charge centers.

Keywords: Alkali cations; Amino acids; Bond dissociation energies; Guided ion beam mass spectrometry; Hydration

1. Introduction

Alkali metals are known to play an important role in the activity of certain enzymes [1]. An example of this is the active site in inosine monophosphate dehydrogenase (IMPDH) [2], where the interaction of a sodium cation with the backbone carbonyl groups of amino acids in the active site loop makes the active site available only to specific substrates. In general, alkali metals ions are found to bond to polar groups such as carbonyl, hydroxyl, carboxylate, amide, and water [3] with few exceptions of binding to "hydrophobic" or "nonpolar" groups [4]. Better understanding of the thermodynamics of these kinds of interactions should improve our ability to understand biomolecular properties in vivo.

Because detailed studies of such complex systems are difficult, studies of simpler systems that contain parts of the biologically relevant interactions should be useful and provide a solid foundation from which to conduct further studies of the more complex systems. Accurate thermodynamic information on the non-covalent interactions between alkali metal ions and amino acids and water molecules have been obtained in our lab and elsewhere [5–15]. In the present study, we begin to expand our studies to relatively bigger systems, hydration of metalated amino acids/oligopeptides, which will begin to tell us about how metal ion interactions with amino acids/oligopeptides are influenced by solvation. Studies using blackbody infrared radiative dissociation have been conducted by Williams and coworkers [13–15] who have reported kinetic and theoretical data for $M^+Val(H_2O)_x$, $M^+ = Li^+$, Na^+, and K^+, $x = 1$–6. These studies find that two water molecules change the metal binding position of Na^+ to valine from bidentate amide–carbonyl [N,CO] coordination

* Corresponding author. Tel.: +1 801 581 7885; fax: +1 801 581 8433.
E-mail address: armentrout@chem.utah.edu (P.B. Armentrout).

1387-3806/$ – see front matter © 2004 Elsevier B.V. All rights reserved.
doi:10.1016/j.ijms.2004.09.019

to the C terminus. For the lithiated complex, the ground state conformer also has bidentate amide–carbonyl [N,CO] coordination for $x = 0$–2, but three water molecules change the preferred coordination site to the C terminus and stabilize the zwitterion as the ground state conformer.

In our laboratory, we are focusing on determinations of the strengths of molecular interactions between metalated amino acids and water molecules. In addition, we would also like to examine the energetics of the major fragmentation processes, which should provide some experimental structural information. Here, one simple system, sodiated glycine solvated by water molecules, $Na^+Gly(H_2O)_x$, was chosen as the starting point for this series of studies. Previous work in our laboratory has already characterized the binding in Na^+Gly and shown it to be bidentate [N,CO] coordination [8]. Thermodynamic data are obtained by using threshold collision-induced dissociation (TCID) as performed with a guided ion beam tandem mass spectrometer (GIBMS) [8,16–21]. In the present studies, the absolute bond dissociation energies (BDEs) of water to sodium glycine cation and glycine to hydrated sodium cations are measured using competitive TCID methods [19,22]. Complementary structural information about these systems is obtained by theoretical studies.

2. Experimental and computational section

2.1. General experimental procedures

The GIBMS has been previously described in detail [23,24]. Briefly, sodium ions are generated in the ion source chamber using a continuous dc discharge in which argon ions sputter a tantalum boat containing sodium metal [25]. The sodium cations produced are carried by a flow of buffer gas (~10% Ar in He) through a 1 m long flow tube at a rate of 4000–9000 standard cm^3/min, usually at a pressure of 0.4–0.9 Torr. The typical operating conditions of the discharge are 1.6–2 kV and 15–20 mA. At 10 cm downstream from the discharge, neutral glycine ligand is introduced using a temperature controllable heated probe. Water is then introduced about 50 cm from the discharge. The complex ions of interest are formed via three-body associative reactions of Na^+ with the glycine and water ligands in the He flow. The complex ions are thermalized to 300 K (the temperature of the flow tube) both vibrationally and rotationally by undergoing 10^4 to 10^5 collisions with the buffer gases in the 1-m long flow tube [25–28]. Therefore, the rovibrational internal energies of all complex ions when exiting the flow tube can be described by a Maxwell–Boltzmann distribution at 300 K. After exiting the flow tube, the ionic complexes travel through several differentially pumped regions and are accelerated and focused into a 66° magnetic sector momentum analyzer that acts as a mass analyzer. The resulting mass-selected ion beam, $Na^+Gly(H_2O)_x$, $x = 1$–4, is decelerated to a well-defined and variable kinetic energy and injected into a radio frequency octopole ion beam guide [29,30]. The neutral reactant (here, Xe) is introduced into a collision cell that surrounds the octopole. All unreacted complexes as well as ions produced by reactions with the neutral gas are trapped by the octopole and thereafter are mass analyzed using a quadrupole mass filter. All ions are efficiently detected with a 27 kV conversion dynode-secondary electron scintillation detector interfaced with fast pulse counting electronics.

Ions intensities, measured as a function of collision energy, are converted to absolute cross sections as described previously [23]. The absolute uncertainties in cross section magnitudes are estimated to be ±20% and relative uncertainties are approximately ±5%. Laboratory (lab) energies are converted to center-of-mass (CM) energies using the equation $E_{CM} = E_{lab}M/(M + m)$, where M and m are the neutral and ion masses, respectively. All energies cited below are in the CM frame unless otherwise noted. The absolute energy scale and the corresponding full-width at half-maximum (FWHM) of the ion beam kinetic energy distribution are determined by using the octopole as a retarding energy analyzer [23]. The energy distributions are nearly Gaussian and have typical FWHMs of 0.2–0.5 eV (lab) in the present experiments.

It has been shown previously [31] that the pressure of the neutral reactant can influence the shape of TCID cross sections because of the effects of multiple collisions. At low pressure, the cross sections are nearly linearly dependent on the measured pressure [23]. In the present systems, we observe some dependence on Xe pressure for the first dissociation product and an obvious dependence for the secondary and higher products. We attribute this to multiple energizing collisions that lead to an enhanced probability of dissociation reactions. Data free from pressure effects (i.e., at single collision conditions) are obtained by extrapolating to zero reactant pressure, as described previously [31,32].

2.2. Dissociation threshold analysis

To determine threshold energies for endothermic reactions, cross sections are modeled using Eq. (1):

$$\sigma(E) = \sigma_0 \sum_i \frac{g_i(E + E_i - E_0)^n}{E} \quad (1)$$

where σ_0 and n are adjustable parameters, E the relative kinetic energy, E_0 the CID threshold energy, and the summation is over the ro-vibrational states i of the ion having energies, E_i and relative populations g_i, where $\Sigma g_i = 1$. In the present studies, two parallel dissociation channels compete with one another such that we use a variant of Eq. (1) as described in detail elsewhere [19].

$$\sigma_j(E) = \left(\frac{n\sigma_{0,j}}{E}\right) \sum g_i \int_{E_{0,j}-E_i}^{E} \left[\frac{k_j(E^*)}{k_{tot}(E^*)}\right] \times [1 - e^{-k_{tot}(E^*)\tau}](E - \varepsilon)^{n-1}\, d(\varepsilon) \quad (2)$$

Here, $\sigma_{0,j}$ is a scaling factor for channel j, $E_{0,j}$ the CID threshold at 0 K for channel j, τ the experimental time for

dissociation ($\sim 5 \times 10^{-4}$ s in the extended dual octopole configuration [24]), ε the energy deposited in the complex by the collision, and E^* is the internal energy of the energized molecule (EM) after the collision, i.e., $E^* = \varepsilon + E_i$. The term $k_j(E^*)$ is the unimolecular rate constant for dissociation to channel j. This rate constant and $k_{tot}(E^*)$ are defined by Rice–Ramsperger–Kassel–Marcus (RRKM) theory as in Eq. (3) [33]:

$$k_{tot}(E^*) = \sum_j k_j(E^*) = \sum_j \frac{d_j N_j^\dagger(E^* - E_{0,j})}{h\rho(E^*)} \quad (3)$$

where d_j is the reaction degeneracy, $N_j^\dagger(E^* - E_{0,j})$ the sum of ro-vibrational states of the transition state (TS) for channel j at an energy $E^* - E_{0,j}$, and $\rho(E^*)$ is the density of states of the EM at the available energy, E^*.

Several effects, which obscure the interpretation of the data, must be accounted for during data analysis in order to produce accurate thermodynamic information. The first effect involves energy broadening resulting from the thermal motion of the neutral collision gas and the kinetic energy distribution of the reactant ion. This is accounted for by explicitly convoluting the model over both kinetic energy distributions, as described elsewhere in detail [23,34]. The second effect arises from energy randomization into the internal modes of the reaction ion after collision. Dissociation of large molecules with many internal modes may not occur during the time scale of experiment, $\sim 5 \times 10^{-4}$ s (as previously measured by time-of-flight studies [24]). This results in a delayed onset for the CID threshold, a kinetic shift, which becomes more noticeable as the size of the molecule increases. These kinetic shifts are estimated by the incorporation of RRKM theory [33] as in Eq. (2), as described in detail elsewhere [22]. To evaluate the rate constants in Eq. (2), sets of rovibrational frequencies for the EM and all TSs are required. Because the metal ligand interactions in $Na^+Gly(H_2O)_x$ are mainly electrostatic (ion–dipole and ion–induced dipole interactions), the most appropriate model for the TS is a loose association of the ion and neutral ligand fragments. Therefore, the TSs are product-like, such that the TS frequencies are those of the dissociation products. The molecular parameters needed for the RRKM calculation are taken from the ab initio calculations detailed in the next section. The transitional frequencies are treated as rotors, a treatment that corresponds to a phase space limit (PSL) and is described in detail elsewhere [22]. For $Na^+Gly(H_2O)_x$ complexes, the five transitional mode rotors have rotational constants equal to those of the $Na^+Gly(H_2O)_{x-1}$ and H_2O products or $Na^+(H_2O)_x$ and glycine products. The 2-D external rotations are treated adiabatically but with centrifugal effects included [19,35].

The model cross section of Eq. (2) is convoluted with the kinetic energy distribution of the reactants and compared to the data. A nonlinear least-squares analysis is used to provide optimized values for $\sigma_{0,j}$, $E_{0,j}$ and n. The uncertainty associated with $E_{0,j}$ is estimated from the range of threshold values determined from different data sets with variations of vibrational frequencies (±10%) and the parameter n, variations of τ by a factor of 2, and the uncertainty in the absolute energy scale, 0.05 eV (lab).

2.3. Computational details

The systems we examine here have many low-lying conformations. A simulated annealing procedure based on molecular mechanics was used to search for possible stable structures in each system's conformational space [36]. All possible structures identified in this way were further optimized using NWChem [37] at the HF/3-21G level [38,39]. Unique structures for each system that are within about 30 kJ/mol of the lowest energy structure (about 20 for each complex) were further optimized using Gaussian 98 W [40] at the B3LYP/6-31G* level [41,42] with the "loose" keyword to facilitate more rapid convergence. The 10 lowest energy structures obtained from this procedure were then chosen for higher-level geometry optimizations and frequency calculations using the B3LYP/6-31G** and MP2(full)/6-31G** levels of theory [43]. We have shown in previous work that these levels of theory are adequate for accurate structure descriptions [8,12]. Single point energy calculations were carried out for the lowest five or six of these optimized structures at the B3LYP, B3P86, and MP2(full) levels using the 6-311+G(2d,2p) [44] basis set. When used in internal energy determinations or for RRKM calculations, the vibrational frequencies calculated at the B3LYP/6-31G** level were scaled by 0.9646 [45]. Zero-point vibrational energy (ZPE) corrections were determined using these scaled vibrational frequencies. Basis set superposition errors (BSSE) for the MP2(full) calculations were estimated using the full counterpoise method. Previous work [8,46] has indicated that BSSE corrections are small for DFT calculations and hence these were not performed.

3. Results and discussion

3.1. Cross sections for collision-induced dissociation

Experimental cross sections were obtained for the interaction of Xe with $Na^+Gly(H_2O)_x$, $x = 1$–4. Figs. 1–4 show representative data for CID of these complexes. Over the energy ranges examined, the dominant dissociation process for all $Na^+Gly(H_2O)_x$ complexes is the loss of one water molecule in reaction 4.

$$Na^+Gly(H_2O)_x + Xe \rightarrow Na^+Gly(H_2O)_{x-1} + H_2O + Xe \quad (4)$$

The magnitudes of the cross sections for losing one water molecule from $Na^+Gly(H_2O)_x$ do not change appreciably for $x = 1$–4. The primary cross sections rise rapidly at low energy and then begin to level off. For $x = 2$–4, these primary cross

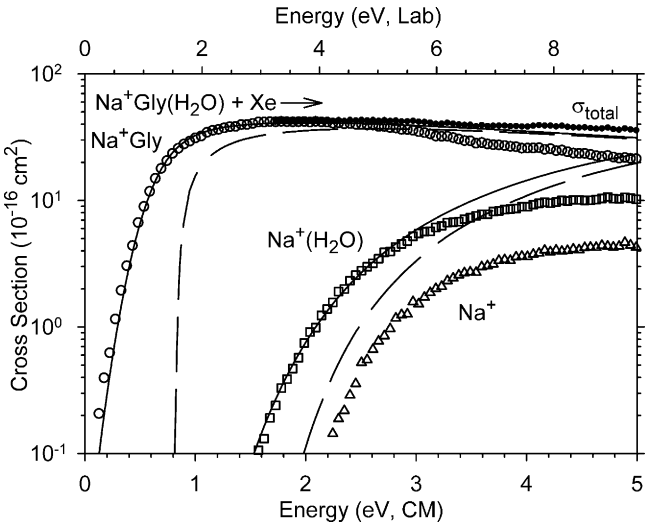

Fig. 1. Zero pressure extrapolated cross sections for CID of $Na^+Gly(H_2O)$ with Xe as a function of kinetic energy in the center-of-mass (lower *x*-axis) and laboratory (upper *x*-axis) frames. The solid lines show the model cross sections of Eq. (2) convoluted over the neutral and ion kinetic and internal energies. The dashed lines show the model cross sections in the absence of experimental kinetic energy broadening for reactants with an internal energy of 0 K.

sections decline at higher energies because of further dissociation of the primary product, as indicated by subsequent losses of water molecules to form $Na^+Gly(H_2O)_{x-y}$, $y = 2$ and 3. The absolute intensities of the ion beams were found to decrease with increasing solvation such that our sensitivity for CID of $Na^+Gly(H_2O)_4$ was rather poor, leading to rather scattered cross sections.

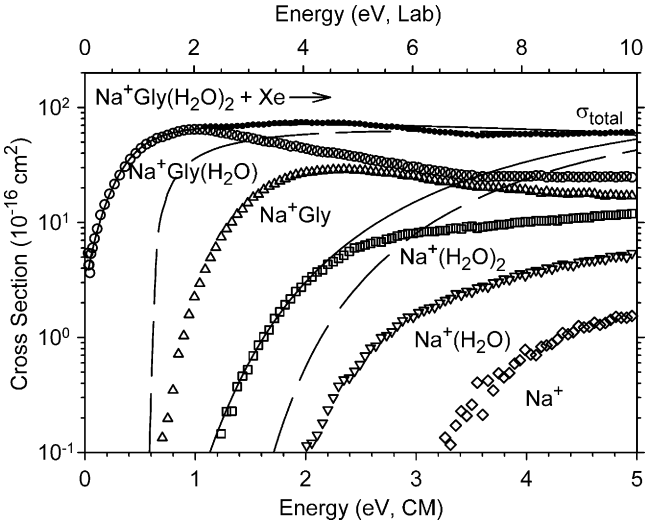

Fig. 2. Zero pressure extrapolated cross sections for CID of $Na^+Gly(H_2O)_2$ with Xe as a function of kinetic energy in the center-of-mass (lower *x*-axis) and laboratory (upper *x*-axis) frames. The solid lines show the model cross sections of Eq. (2) convoluted over the neutral and ion kinetic and internal energies. The dashed lines show the model cross sections in the absence of experimental kinetic energy broadening for reactants with an internal energy of 0 K.

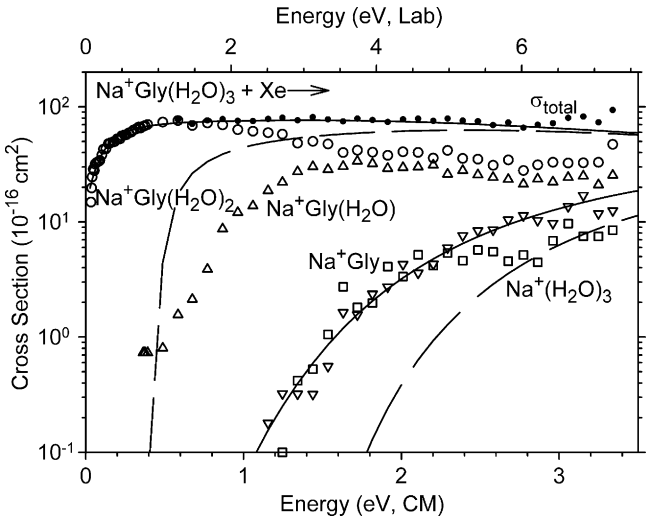

Fig. 3. Zero pressure extrapolated cross sections for CID of $Na^+Gly(H_2O)_3$ with Xe as a function of kinetic energy in the center-of-mass (lower *x*-axis) and laboratory (upper *x*-axis) frames. The solid lines show the model cross sections of Eq. (2) convoluted over the neutral and ion kinetic and internal energies. The dashed lines show the model cross sections in the absence of experimental kinetic energy broadening for reactants with an internal energy of 0 K.

In addition to reaction 4, loss of the glycine ligand is observed in the competitive reaction 5 at higher energies in all cases except $x = 4$.

$$Na^+Gly(H_2O)_x + Xe \rightarrow Na^+(H_2O)_x + Gly + Xe \qquad (5)$$

The $Na^+(H_2O)_x$ cross sections are much smaller than those of the $Na^+Gly(H_2O)_{x-1}$ products and have apparent thresholds that are more than 1 eV higher. This indicates that

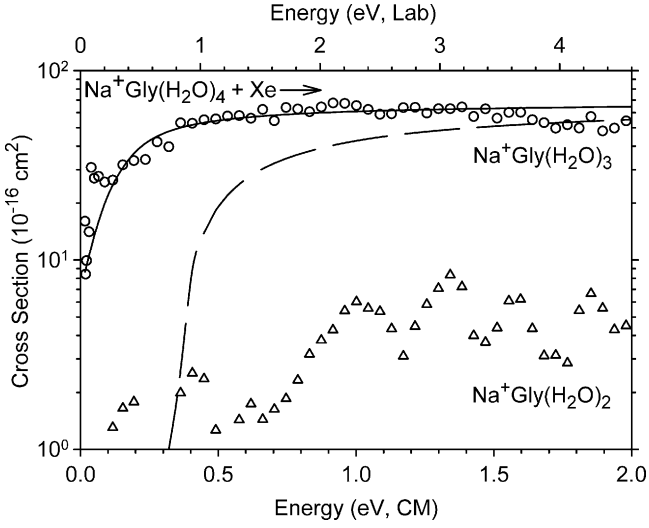

Fig. 4. Zero pressure extrapolated cross sections for CID of $Na^+Gly(H_2O)_4$ with Xe as a function of kinetic energy in the center-of-mass (lower *x*-axis) and laboratory (upper *x*-axis) frames. The solid line shows the model cross section of Eq. (2) convoluted over the neutral and ion kinetic and internal energies. The dashed line shows the model cross section in the absence of experimental kinetic energy broadening for reactants with an internal energy of 0 K.

the interaction between glycine and Na^+ is stronger than that of H_2O and Na^+, consistent with previous measurements, $D_0(Na^+\text{-Gly}) = 164 \pm 6$ kJ/mol and $D_0(Na^+\text{-}H_2O) = 95 \pm 8$ kJ/mol [6,8]. Loss of water molecules from the $Na^+(H_2O)_x$ products were also found for $x = 1$–3. In no system was a ligand exchange process forming a Xe containing species observed.

3.2. Threshold analysis and results

We have shown previously [19,47] that the best measurement of the thresholds for competitive dissociation processes comes from the simultaneous analysis of the cross sections. Otherwise thresholds for the higher energy process are elevated from their thermodynamic values as a consequence of competition with the lower energy channel. The constraints imposed by this simultaneous analysis lead to relatively precise threshold values compared with analyses of the individual channels. The competitive model of Eq. (2) was used to analyze the competitive processes 4 and 5 for $Na^+Gly(H_2O)_x$ systems with $x = 1$–3. For $Na^+Gly(H_2O)_4$, the weak ion intensity did not permit observation of the competitive channel, $Na^+(H_2O)_4$, therefore, Eq. (2) with only one channel ($k_j = k_{tot}$) was used to model its cross section. Figs. 1–4 show that all experimental cross sections are reproduced well by Eq. (2) over energy ranges of 1–3 eV. The optimized parameters of Eq. (2) are reported in Table 1 along with results from previous work on dissociation of the Na^+Gly complex [8]. The ideal way of modeling the competitive cross sections should be to use a common scaling factor, $\sigma_{0,j} = \sigma_0$, for both channels [19,47]. However, the use of a common scaling factor fails to reproduce the data for $x = 1$ and 2, perhaps because important factors (e.g., reaction degeneracies, symmetry numbers of the reactant and product molecules, neutral products' dipole moments, inaccurate estimations of metal ligand frequencies) are neglected when modeling the experimental cross sections. Therefore, independent scaling factors were introduced for these two systems. This added flexibility negligibly changes the final absolute bond energies for the lower energy threshold channel as compared to results obtained using a common scaling factor. For the higher energy channel, use of a common scaling factor leads to thresholds that decrease by less than 0.1 eV, however, the quality of the fits is considerably poorer than those obtained using independent scaling factors. The trend in the final BDEs is illustrated in Fig. 5. The experimental BDEs for losing water or glycine decrease monotonically with increasing number of water molecules. The BDE for losing glycine is larger than that for losing water from each $Na^+Gly(H_2O)_x$ complex, $x = 1$–4, consistent with the qualitative dissociation behavior.

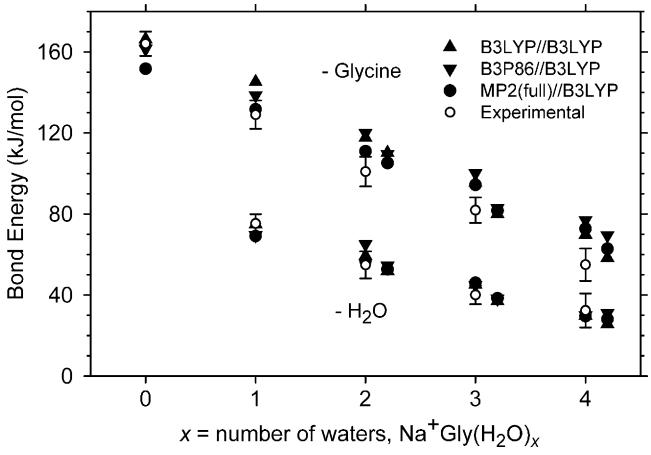

Fig. 5. Comparison of experimental (open symbols) and theoretical (closed symbols) bond dissociation energies (in kJ/mol) for loss of H_2O and Gly from $Na^+Gly(H_2O)_x$, $x = 0$–4, complexes. Values for the MP2(full)//MP2(full) calculations are not shown for clarity but are essentially identical to those for MP2(full)//B3LYP. Values shown in-line with the experimental values are the adiabatic calculated values, whereas the diabatic BDEs discussed in the text are shown displaced to the right.

The results in Table 1 were obtained using molecular parameters for the ground state structures calculated at the B3LYP/6-31G** level in all cases (see next section). We also checked whether using different molecular structures for the $Na^+Gly(H_2O)_x$, $x = 2$–4, complexes changed any of the fitting parameters. In all cases, values for $\sigma_{0,j}$, n, and $E_{0,j}$ were

Table 1
Fitting parameters for Eq. (2) and entropies of activation at 1000 K

Reactant	Ionic product	d_j[a]	$\sigma_{0,j}$	n	$E_{0,j}$ (eV)	$\Delta S^{\ddagger}_{1000}$[b] (J/(mol K))
Na^+Gly[c]	Na^+	1	20 (4)	1.1 (0.1)	1.70 (0.05)	40 (5)
$Na^+Gly(H_2O)$	Na^+Gly	0.5	63 (4)	0.9 (0.1)	0.78 (0.05)	−7 (1)
	$Na^+(H_2O)$	0.5	20 (4)		1.34 (0.07)	30 (1)
$Na^+Gly(H_2O)_2$	$Na^+Gly(H_2O)$	0.5	88 (4)	1.0 (0.1)	0.57 (0.07)	26 (1), 6 (1)
	$Na^+(H_2O)_2$	0.5	23 (9)		1.05 (0.08)	66 (2), 46 (2)
$Na^+Gly(H_2O)_3$	$Na^+Gly(H_2O)_2$	0.5	83 (5)	1.0 (0.1)	0.41 (0.05)	6 (1), 20 (1)
	$Na^+(H_2O)_3$	0.33	83 (5)		0.85 (0.07)	65 (1), 79 (1)
$Na^+Gly(H_2O)_4$	$Na^+Gly(H_2O)_3$	0.5	66 (1)	1.0 (0.1)	0.34 (0.09)	52 (1), 50 (1)

Uncertainties are listed in parentheses.
[a] Reaction degeneracy: defined as the ratio of rotational symmetry numbers of the reactant to the products in the PSL TS.
[b] First and second values listed are for the adiabatic and diabatic, respectively, pathways discussed in the text.
[c] From Moison and Armentrout [8].

Table 2
Relative energies of $Na^+Gly(H_2O)_x$ in kJ/mol

Complex	Structure	Level of theory			
		B3LYP[a]	B3P86[a]	MP2(full)[a]	MP2(full)[b]
$Na^+Gly(H_2O)$	1W-M1[N,CO]	0	1.5	0	0
	1W-M6[CO]	5.4	0	7.9	–[c]
	1W-M3[CO,OH]	6.5	1.1	5.8	5.8
	1W[bOH]-M6[CO]	9.6	2.9	7.8	7.6
	1W-ZW[CO_2^-]	14.2	5.8	10.3	10.1
$Na^+Gly(H_2O)_2$	2W[bOH]-M6[CO]	0	0	0	0
	2W-M1[N, CO]	7.4	10.6	4.2	3.9
	2W-M3[CO,OH]	8.2	10.3	8.4	7.1
	2W[bN]-M9[CO]	9.5	9.2	7.6	8.0
	2W[bO$^-$]-ZW[CO]	11.0	9.8	9.9	10.6
$Na^+Gly(H_2O)_3$	3W[bOH]-M6[CO]	0	0	0	0
	3W[bN]-M9[CO]	7.3	8.5	6.0	6.5
	3W[NH,bO$^-$]-ZW[CO]	10.2	7.6	12.8	13.6
	3W-M1[N,CO]	15.5	17.3	9.3	9.5
	3W[bCO]-M3[OH]	16.7	15.9	14.3	13.5
	3W[bO$^-$]-ZW[CO]	17.1	15.9	17.3	17.4
$Na^+Gly(H_2O)_4$	4W[bOH,bOH_2]-M6[CO]	0	2.0	6.7	7.9
	4W[2NH,bO$^-$]-ZW[CO]	0.9	0	7.9	9.8
	4W[bOH,bCO]-M6[CO]	1.3	4.0	0	0
	4W[NH,bO$^-$]-ZW[CO]	2.4	2.5	7.5	9.6
	4W[bOH]-M6[CO]	2.6	5.7	3.7	11.3
	4W[bN]-M9[CO]	12.7	11.4	7.5	7.7
	4W[bCO,bO$^-$]-ZW[CO]	19.0	18.3	16.9	18.8

Includes zero point energy corrections for all values.
[a] Structures optimized at the B3LYP/6-31G** level. All single point energies are calculated using the 6-311 + G(2d,2p) basis set at the indicated level of theory.
[b] Relative energies calculated at the MP2(full)/6-311 + G(2d,2p)//MP2(full)/6-31G** level.
[c] 1W-M6[CO] collapses to 1W-M3[CO,OH] at this level of calculation.

essentially unchanged (e.g., thresholds for water loss were the same and those for glycine loss changed by less than 0.01 eV). The only factors that did change appreciably were the $\Delta S^{\ddagger}_{1000}$ values. As will be discussed below, it is possible that alternate structures (M1[N,CO] for $x = 2$–3 and M9[CO] for $x = 4$) are the species produced experimentally. If molecular parameters for these structures are used in the data analysis, $\Delta S^{\ddagger}_{1000}$ values for water loss are 6, 20, and 50 J/(mol K) and 46 and 79 J/(mol K) for glycine loss. No matter what molecular parameters are used, we find that the entropy of activation for water loss is much smaller (by 40–60 J/(mol K)) than for glycine loss, which reflects the constraints on the torsional motions of glycine when complexed to Na^+.

3.3. Theoretical results

As described above, all structures for $Na^+Gly(H_2O)_x$ and their products were optimized at the B3LYP/6-31G** and MP2(full)/6-31G** levels of theory. Both levels of theory predict the same low energy structures for $x = 1$–4 in Table 2. The five lowest energy structures optimized at the B3LYP/6-31G** level for $Na^+Gly(H_2O)_x$, $x = 1$–4, are displayed in Figs. 6–9. For discussion purposes, one additional optimized structure is included for $x = 3$ and 4 in Figs. 8 and 9, respectively. The single point energy values including zero point energy (ZPE) corrections calculated at four different levels of theory relative to the ground state energy are given in Table 2. All relative energies mentioned below list the range of results at these four levels if not otherwise specified.

To identify the structures of the complex, we use nomenclature that starts with the nomenclature established previously for Na^+Gly [8]. The zwitterion is designated as ZW and nonzwitterionic structures as M*y* (where the *y* refers to a specific structure as first designated by Jensen [48]). The notation in brackets after these describes the sodium binding site for each conformer. The *x*W before ZW or M*y* indicates the number of water molecules attached to Na^+Gly, and the notation in brackets after *x*W indicates the water binding site unless the water molecule simply binds directly to the sodium ion through the oxygen atom. Several important geometric parameters for the $Na^+Gly(H_2O)_x$ complexes are provided in Table 3. All calculated BDEs for adiabatic and diabatic processes (see discussion below) along with the experimental ones are listed in Table 4 and their trends are displayed in Fig. 5. For comparison purposes, we optimized the five lowest energy structures of Na^+Gly at the same levels of theory used here, B3LYP/6-31G** and MP2(full)/6-31G**, and include these results in Tables 3 and 4 as well. These structures and their relative energies are comparable to those elucidated previously [8] at the MP2(full)/6-31G* level.

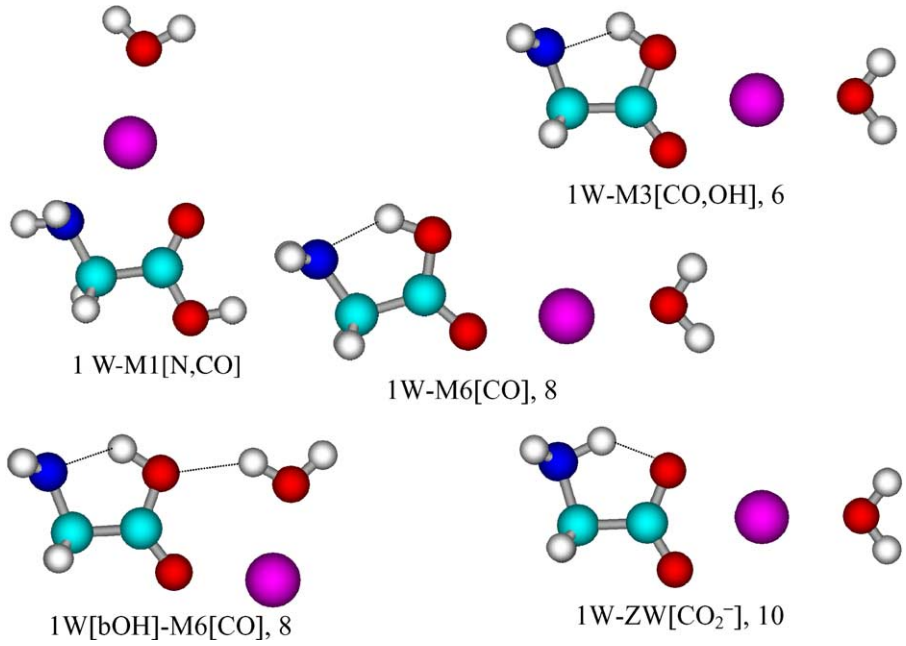

Fig. 6. Optimized structures and relative energies (in kJ/mol) of $Na^+Gly(H_2O)$ calculated at the MP2(full)/6-311 + G(2d,2p)//B3LYP/6-31G** level.

3.4. Na^+Gly and $Na^+Gly(H_2O)$

As reported elsewhere [8,49], Na^+ favors [N,CO] coordination to nonzwitterionic glycine in the gas phase, and the current calculations yield the same result. Here, we find that for both Na^+Gly and $Na^+Gly(H_2O)$, Na^+ binds in a bidentate configuration to the amino nitrogen and carbonyl oxygen, M1[N,CO], and is approximately aligned with the axis of the molecular dipole of glycine in this conformation. The calculations predict an almost identical glycine backbone structure for the ground state structures in both cases, Table 3. The Na^+–O=C and Na^+–N distances for $Na^+Gly(H_2O)$ are elongated compared to those of Na^+Gly. These bond lengths increase by 0.032 and 0.028 Å, respectively, from $x = 0$ to 1, while the $\angle Na^+$–O=C bond angle stays about the same (Table 3). Clearly electron delocalization from the water molecule to Na^+ weakens the binding to glycine. All levels of theory (Table 2) predict the same ground conformer, 1W-M1[N,CO], for $Na^+Gly(H_2O)$, except B3P86 which predicts that 1W-M6[CO] is 1.5 kJ/mol lower. The 1W-M6[CO] structure is stable for DFT calculations but collapses to 1W-M3[CO,OH] when optimized at the MP2(full)/6-31G** level, similar to results for Na^+Gly [8]. The sodium ion in 1W-M3[CO,OH] does not align with the dipole of glycine in this conformation very well, but this energetic disadvantage is offset by better interaction with the hydroxyl oxygen. 1W[bOH]-M6[CO], where the water molecule bridges to the hydroxyl oxygen and forms a pseudo-six member ring with the carboxylic group and sodium ion, Fig. 6, is also predicted to be a stable structure and lies 3–10 kJ/mol higher than the ground conformer, 1W-M1[N,CO].

All levels of theory find that one of the five lowest energy structures for $Na^+Gly(H_2O)$ is the zwitterion, 1W-ZW[CO_2^-] where the sodium ion coordinates to both oxygen atoms of the carboxylate group of glycine. The zwitterion is located 6–14 kJ/mol higher than the ground conformer and 4–8 kJ/mol higher than its corresponding 1W-M3[CO,OH] nonzwitterion. Our calculations of Na^+Gly find that ZW[CO_2^-] is located only 6–10 kJ/mol higher than the M1[N,CO] ground conformer and −2 to 1 kJ/mol lower than M3[CO,OH]. Thus, addition of water to Na^+Gly slightly destabilizes the zwitterion and stabilizes its corresponding nonzwitterion compared to the ground conformer. This is mainly because electron delocalization from water to Na^+ reduces the electrostatic interaction between the sodium ion and the carboxylate group (as evidenced by the increase in the Na^+–O=C distance, Table 3), which results in less stabilization of the negative charge on the carboxylate group.

3.5. $Na^+Gly(H_2O)_2$

For $Na^+Gly(H_2O)_2$, four different levels of theory predict the same ground conformer, 2W[bOH]-M6[CO], Fig. 7, which can be regarded as the combination of hydration in 1W-M6[CO] and 1W[bOH]-M6[CO], Fig. 6. Clearly, attachment of the second water molecule changes the most favorable sodium binding site from [N,CO] coordination to C=O coordination at the carbonyl. This avoids twisting the glycine backbone compared to the deformations in Na^+Gly and $Na^+Gly(H_2O)$, as indicated in Table 3 by the N–C–C=O dihedral angles, 14.5°, 14.1°, and 180° for $x = 0$–2, respectively. Addition of a second water molecule has also been

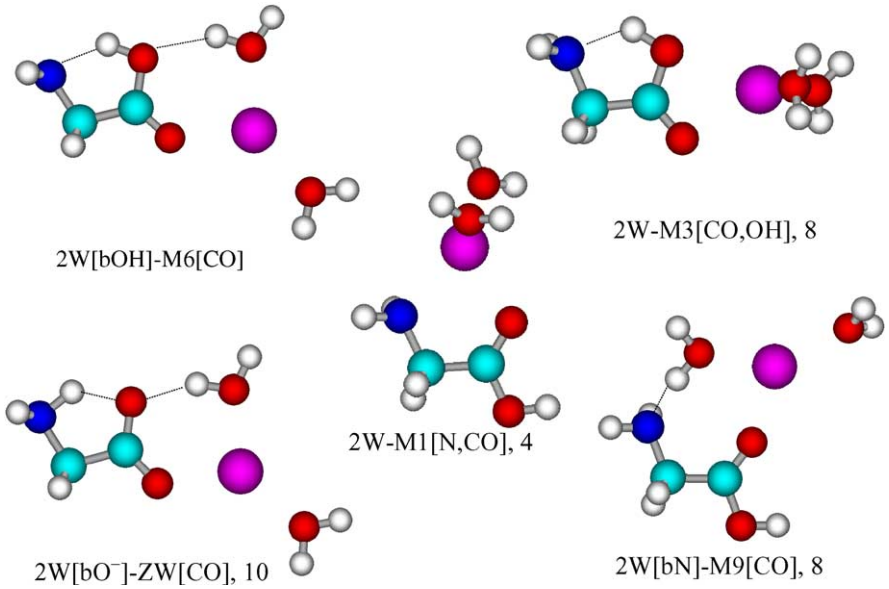

Fig. 7. Optimized structures and relative energies (in kJ/mol) of $Na^+Gly(H_2O)_2$ calculated at the MP2(full)/6-311 + G(2d,2p)//B3LYP/6-31G** level.

found to change the preferred binding site from [N,CO] coordination to C=O coordination in the case of hydrated valine sodium cation complexes [13,14]. Recent calculations by Ai and Bu [50] at the B3LYP/6-31G* level also indicate that the most stable structure of doubly hydrated Glycine-H^+Na^+ is C=O coordination of glycine to sodium ion with one of the water molecules bridging to the hydroxyl.

Among the five lowest energy geometries of $Na^+Gly(H_2O)_2$, Fig. 7, 2W-M1[N,CO] maintains the [N,CO] coordination found in the $Na^+Gly(H_2O)$ and Na^+Gly ground state structures with a similar glycine backbone geometry (compare $\angle Na^+–O=C$ bond angles and the $\angle Na^+–O=C–C$ and $\angle N–C–C=O$ dihedral angles in Table 3). This structure is located 4–11 kJ/mol higher than the 2W[bOH]-M6[CO], global minimum. The reversal in the relative energies of the M1[N,CO] and M6[CO] structures from $x = 1$ to 2 probably results from the removal of the structural constraints on neutral glycine (N–C–C=O dihedral angles noted above) and a better separation of water molecules in 2W[bOH]-M6[CO] than in 2W-M1[N,CO] ($\angle C=O–Na^+–OH_2$ dihedral angles, Table 3). We believe that a key factor in this reversal can be understood on the basis of the "dissection" of the pairwise interactions in Na^+Gly, as elucidated previously [8]. Here, we showed that the most favorable binding site for Na^+ to a single functional group is the carbonyl with a nearly linear $Na^+–O=C$ bond an-

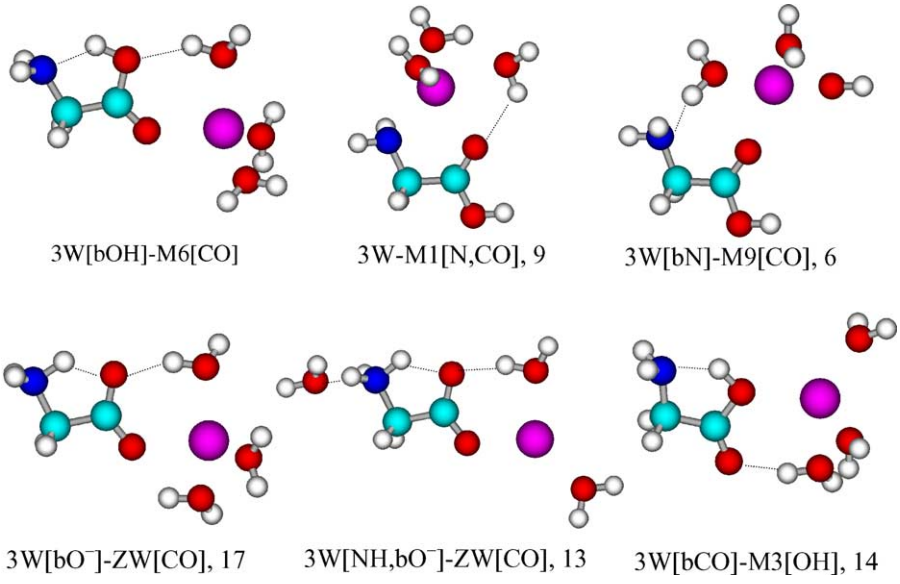

Fig. 8. Optimized structures and relative energies (in kJ/mol) of $Na^+Gly(H_2O)_3$ calculated at the MP2(full)/6-311 + G(2d,2p)//B3LYP/6-31G** level.

gle. The M6[CO] structure achieves this binding site, but the M1[N,CO] structure is thermodynamically preferred because glycine utilizes bidentate binding. However, once two water molecules are added, the sodium ion can bind in a much more optimal position to the carbonyl, while also delocalizing electron density to the hydroxyl through the water bridge in the 2W[bOH]-M6[CO] structure.

Another nonzwitterionic structure, 2W[bN]-M9[CO], is located 8–10 kJ/mol higher than the global minimum. Here, the Na^+ interacts with the carbonyl group and a water molecule bridges to nitrogen. This again allows better alignment of the Na^+ with the preferred carbonyl binding site, while retaining electron delocalization with the NH_2 group through the water bridge. Note that the water bridge also allows the H–C–N–H dihedral angle to move to 52.8° from the 38.2° angle in 2W-M1[N,CO], which removes some of the strain of partially eclipsed CH and NH bonds to hydrogen. The calculations also predict that the 2W[bO$^-$]-ZW[CO] zwitterion of $Na^+Gly(H_2O)_2$ is one of the five lowest energy structures. Here, Na^+ interacts with the C terminus of glycine similar to the 1W-ZW[CO_2^-] zwitterion of $Na^+Gly(H_2O)$. Four levels of theory predict that it is 10–11 kJ/mol less stable than its corresponding nonzwitterionic conformation, 2W[bOH]-M6[CO], the ground state structure. For the reasons discussed above, the energy difference between the corresponding nonzwitterionic and zwitterionic forms increases from 4 to 8 kJ/mol for $Na^+Gly(H_2O)$ to 10–11 kJ/mol for $Na^+Gly(H_2O)_2$.

3.6. $Na^+Gly(H_2O)_3$

Similar to the doubly hydrated complex, the ground structure of $Na^+Gly(H_2O)_3$, 3W[bOH]-M6[CO] (Fig. 8), has the sodium ion coordinating to the carbonyl group of glycine with one of the water molecules hydrogen bonding to the hydroxyl group. All four levels of theory (Table 2) predict this as the ground state. The additional water adds in a position such that the Na^+ ion is nearly tetrahedrally coordinated. The Na^+–O=C distance in $Na^+Gly(H_2O)_x$ increases from 2.247 Å for $x = 2$ to 2.295 Å for $x = 3$ and the average Na^+–OH_2 bond distance increases from 2.224 to 2.261 Å, consistent with weakening of the bonds. The structure that has the same binding pattern as the ground conformers of $Na^+Gly(H_2O)$ and Na^+Gly, 3W-M1[N,CO], is 9–17 kJ/mol higher than the global minimum largely because of steric crowding around the five-coordinate Na^+ ion. The structure, 3W[bN]-M9[CO], is located 6–9 kJ/mol higher than the ground conformer but 3–9 kJ/mol lower than the [N,CO] coordinated structure. The Na^+–N, Na^+–O=C, and average Na^+–OH_2 bond distances are 0.025, 0.047 and 0.043 Å (Table 3) longer than those in 2W[bN]-M9[CO] because of the additional hydration on Na^+. The reversal in the relative energies of the M1[N,CO] and M9[CO] structures from $x = 2$ to 3 is again related to steric crowding in the former. In 3W[bCO]-M3[OH], which lies 13–17 kJ/mol above the ground conformer, the Na^+ attaches to the hydroxyl oxygen and uses a water bridge back to the CO group, a much less favorable geometry as shown by "dissection" of Na^+Gly [8].

Our calculations show that the 3W[NH,bO$^-$]-ZW[CO] zwitterion (Fig. 8) is one of the five lowest energy structures and lies 7–14 kJ/mol above the ground state. The zwitterionic analogue of the ground conformer 3W[bO$^-$]-ZW[CO] (Fig. 8) is located 4–8 kJ/mol higher than 3W[NH,bO$^-$]-ZW[CO]. Clearly, attachment of the third water to the $Na^+Gly(H_2O)_2$ zwitterion has a preference for binding at the NH_3^+ charge center compared to the Na^+ charge site, because the former avoids a more crowded population of water molecules around the sodium ion. As mentioned above,

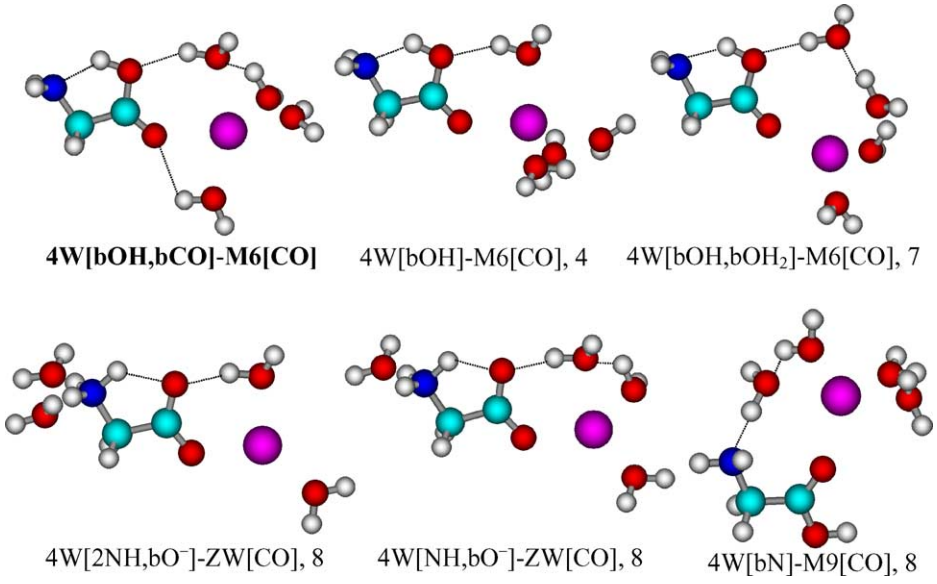

Fig. 9. Optimized structures and relative energies (in kJ/mol) of $Na^+Gly(H_2O)_4$ calculated at the MP2(full)/6-311 + G(2d,2p)//B3LYP/6-31G** level.

Table 3
Geometrical parameters of $Na^+Gly(H_2O)_x$ structures optimized at B3LYP/6-31G**

Species[a]	$r(Na^+—N)$ (Å)	$r(Na^+—O{=}C)$ (Å)	$r(Na^+—OH_2)$ (Å)	$\angle Na^+—O{=}C$ (°)	$\angle Na^+—O{=}C—C$ (°)	$\angle N—C—C{=}O$ (°)	$\angle C{=}O—Na^+—OH_2$ dihedral (°)
M1[N,CO]	2.421	2.216	–		1.6	14.5	–
ZW[CO_2^-]	–	2.257	–	89.0	180.0	180.0	–
M3[CO,OH]	–	2.255	–	97.5	180.0	180.0	–
M4[N,CO]	2.449	2.196	–	120.5	3.2	13.6	–
M5[N,OH]	2.368	4.338	–	15.1	174.7	153.2	–
1W-M1[N,CO]	2.449	2.248	2.228	117.9	3.3	14.1	176.9
1W-M6[CO]	–	2.178	2.217	131.0	180.0	180.0	179.2
1W-M3[CO,OH]	–	2.284	2.218	97.7	179.9	180.0	179.1
1W[bOH]-M6[CO]	–	2.211	2.188	131.8	180.0	180.0	0.0
1W-ZW[CO_2^-]	–	2.285	2.229	89.3	180.0	180.0	177.9
2W[bOH]-M6[CO]	–	2.247	2.212, 2.235	133.2	180.0	180.0	0.0, 179.8
2W-M1[N,CO]	2.472	2.290	2.260, 2.262	117.5	6.5	13.8	100.3, 128.2
2W-M3[CO,OH]	–	2.315	2.244, 2.246	98.7	179.9	179.7	104.7, 108.6
2W[bN]-M9[CO]	3.825	2.245	2.173, 2.238	150.5	44.8	6.7	24.9, 153.8
2W[bO^-]-ZW[CO]	–	2.233	2.192, 2.242	125.3	180.0	179.9	0.0, 180.0
3W[bOH]-M6[CO]	–	2.295	2.259, 2.261, 2.263	133.4	176.8	179.7	2.8, 107.2, 126.6
3W[bN]-M9[CO]	3.850	2.292	2.215, 2.263, 2.269	147.8	54.3	2.5	28.2, 82.9, 151.3
3W[NH,bO^-]-ZW[CO]	–	2.218	2.195, 2.245, 1.735[b]	124.1	178.1	178.5	0.8, 136.3, 177.4
3W-M1[N,CO]	2.484	2.397	2.274, 2.276, 2.411	117.8	3.6	12.3	94.0, 102.0, 165.0
3W[bCO]-M3[OH]	–	3.407	2.229, 2.250, 2.297	73.9	176.6	179.5	72.1, 117.1, 177.9
3W[bO^-]-ZW[CO]	–	2.258	2.251, 2.253, 2.357	126.9	176.9	179.7	4.0, 65.9, 136.5
4W[bOH,bOH_2]-M6[CO]	–	2.246	2.246, 2.257, 2.314, 3.954	157.1	174.8	179.6	10.2, 14.8, 68.5, 150.8
4W[2NH,bO^-]-ZW[CO]	–	2.208	2.202, 2.247, 1.788[b], 1.789[b]	123.0	178.7	178.4	1.4, 129.0, 135.9, 177.9
4W[bOH,bCO]-M6[CO]	–	2.409	2.252, 2.292, 2.386, 2.415	136.8	177.1	179.8	4.7, 62.0, 66.4, 177.3
4W[NH,bO^-]-ZW[CO]	–	2.242	2.361, 2.255, 2.265, 1.737[b]	126.1	178.1	179.4	3.4, 65.4, 131.9, 137.6
4W[bOH]-M6[CO]	–	2.336	2.251, 2.271, 2.422, 2.462	134.4	170.4	179.7	15.4, 117.6, 130.2, 165.9
4W[bN]-M9[CO]	3.895	2.317	2.258, 2.315, 2.365, 2.386	149.6	57.9	2.2	28.3, 90.8, 93.2, 168.5
4W[bCO,bO^-]-ZW[CO]	–	2.393	2.278, 2.293, 2.402, 2.418	130.6	173.9	179.7	7.1, 63.8, 67.6, 174.3

[a] Names and numbers in bold indicate the lowest energy structures.
[b] The $NH—OH_2$ distance.

Table 4
Calculated H_2O and glycine binding energies (kJ/mol) for $Na^+Gly(H_2O)_x$ at 0 K

Reactant	Ionic product	Experiment	H_2O and glycine binding energy (kJ/mol)			
			B3LYP[a]	B3P86[a]	MP2(full)[a]	MP2(full)[b]
M1[N,CO]	Na^+	164.0 (6)[c]	166.2	161.5	151.7	152.1
1W-M1[N,CO]	M1[N,CO]	75.3 (5)	74.9	69.5	69.1	69.3
	$Na^+(H_2O)$	129.0 (7)	145.2	138.5	131.7	131.4
2W[bOH]-M6[CO]	1W-M1[N,CO]	54.9 (7)	59.3	65.1	57.0	57.4
	$Na^+(H_2O)_2$	100.9 (7)	117.7	120.0	111.0	110.5
2W[bOH]-M1[N,CO]	1W-M1[N,CO]	54.9 (7)	51.9	54.5	52.7	53.5
	$Na^+(H_2O)_2$	100.9 (7)	110.2	109.5	105.2	106.0
3W[bOH]-M6[CO]	2W[bOH]-M6[CO]	40.0 (5)	45.2	44.8	46.0	47.3
	$Na^+(H_2O)_3$	81.9 (6)	95.6	100.1	94.4	95.4
3W[bOH]-M1[N,CO]	2W[bOH]-M1[N,CO]	40.0 (5)	37.0	38.1	38.4	40.8
	$Na^+(H_2O)_3$	81.9 (6)	80.0	82.8	81.7	82.1
4W[bOH,bCO]-M6[CO]	3W[bOH]-M6[CO]	32.4 (8)	29.8	29.9	29.6	32.1
	$Na^+(H_2O)_4$	55.0 (8)	69.8	76.9	72.7	65.6
4W[bN]-M9[CO]	3W[bOH]-M1[N,CO]	32.4 (8)	33.9	39.8	33.0	34.4
	$Na^+(H_2O)_4$	55.0 (8)	58.3	69.4	62.8	65.0
MAD(adiabatic)[d]	$-H_2O$		3.2 (2)	5.8 (3)	4.3 (2)	4.0 (3)
	−Gly		12.7 (6)	14.2 (8)	11.1 (5)	9.6 (4)
MAD(diabatic)[e]	$-H_2O$		2.0 (1)	3.9 (3)	2.7 (2)	2.6 (2)
	−Gly		6.6 (6)	7.2 (5)	5.5 (5)	5.9 (5)

Including ZPE corrections for all and BSSE corrections for MP2(full).
[a] Energies calculated at the indicated level with 6-311 + G(2d,2p) basis and B3LYP/6-31G** geometries.
[b] Energies calculated at the MP2(full)/6-311 + G(2d,2p)//MP2(full)/6-31G** level.
[c] Moision and Armentrout [8].
[d] Mean absolute deviation from the experimental values for the calculated adiabatic processes.
[e] Mean absolute deviation from the experimental values for the calculated diabatic processes.

continuing solvation on sodium ion of the complex (thus decreasing the effective charge on the sodium ion), such as 3W[bO^-]-ZW[CO], does reduce its ability to stabilize the negative carboxylate group of the complex. As for the smaller complexes, the ZW continues to be destabilized relative to the nonZW as the sodium ion becomes more highly solvated.

3.7. $Na^+Gly(H_2O)_4$

The $Na^+Gly(H_2O)_4$ ground state structure is predicted to be 4W[bOH,bOH_2]-M6[CO] by B3LYP, 4W[2NH,bO^-]-ZW[CO] by B3P86, and 4W[bOH,bCO]-M6[CO] by MP2(full), Table 2 and Fig. 9. All of these conformations retain carbonyl coordination of glycine to Na^+ and relatively small distortions from the neutral glycine structure as in the ground state structures of $Na^+Gly(H_2O)_2$ and $Na^+Gly(H_2O)_3$. For 4W[bOH,bCO]-M6[CO], the Na^+–O=C distance in $Na^+Gly(H_2O)_x$ increases from 2.295 Å for $x = 3$ to 2.409 Å for $x = 4$, the average Na^+–OH_2 bond distance increases from 2.261 to 2.336 Å, and the ∠Na^+–O=C bond angle increases from 133.4° to 136.8°. However, for 4W[bOH,bOH_2]-M6[CO], there is less steric congestion around Na^+ as only three waters solvate the sodium ion, which is nearly tetrahedrally coordinated, with another water molecule bridging to the hydroxyl oxygen. In this case, the Na^+–O=C distance is 2.246 Å, 0.163 Å shorter than that of 4W[bOH,bCO]-M6[CO], and the average Na^+–OH_2 bond distance (exclude the bridging water that does not interact with sodium ion directly) is 0.064 Å shorter than in 4W[bOH,bCO]-M6[CO]. The ∠Na^+–O=C bond angle is 20.3° larger than that of 4W[bOH,bCO]-M6[CO], which indicates that the sodium ion can align with the carbonyl better, but delocalization to the hydroxyl group is worse as it now involves a two water bridge. The 4W[2NH,bO^-]-ZW[CO] retains the structure of 2W[bO^-]-ZW[CO] for $Na^+Gly(H_2O)_2$ with the additional two water molecules solvating the $-NH_3^+$ group of glycine. Comparison of the geometries of the 4W[2NH,bO^-]-ZW[CO] and 2W[bO^-]-ZW[CO] structures finds them to be similar, Table 3, except for the Na^+–O=C distance, which is 0.025 Å shorter in the four water complex, and the NH–O hydrogen bond, which is 0.223 Å longer in the four water complex. This implies that solvation of the NH_3^+ charge center by two water molecules leads to less electron density donated from CO_2^- to NH_3^+, such that more is available for delocalization to Na^+. This same trend is also seen when only a single water hydrates the $-NH_3^+$ group in the 4W[NH,bO^-]-ZW[CO] complex, where the NH–O hydrogen bond is 0.140 Å longer than in 2W[bO^-]-ZW[CO]. Here, the Na^+–O=C bond is

0.009 Å longer than in 2W[bO$^-$]-ZW[CO], a result of the enhanced hydration at the Na^+ site by a third water molecule.

All levels of theory show that another three structures of $Na^+Gly(H_2O)_4$ are located only a few kJ/mol above the ground state structure. 4W[bOH]-M6[CO] is located 2–11 kJ/mol higher than the 4W[bOH,bCO]-M6[CO] ground state. These two conformers have similar structures with slightly different arrangements of the water molecules, and fewer hydrogen bonds in the higher energy structure. The 4W[bN]-M9[CO] structure lies 7–13 kJ/mol higher than the ground state and appears destabilized by steric crowding at the five-coordinate Na^+, Fig. 9. One of the stable zwitterionic structures, 4W[NH,bO$^-$]-ZW[CO], is only 1–10 kJ/mol higher than the most stable charge solvated structure. Similar to the most stable zwitterion of $Na^+Gly(H_2O)_3$, one of the water molecules in 4W[NH,bO$^-$]-ZW[CO] binds to the NH_3^+ instead of the sodium ion, and the other three water molecules bind directly to sodium ion; among these, one is hydrogen bonding to the other oxygen of the carboxylate group. Another zwitterion, 4W[bCO,bO$^-$]-ZW[CO] (not shown in Fig. 9), is located 14–19 kJ/mol higher than its corresponding nonzwitterion 4W[bOH,bCO]-M6[CO], and 9–18 kJ/mol higher than 4W[2NH,bO$^-$]-ZW[CO], which indicates the fourth water molecule has a strong preference for binding at the NH_3^+ charge center compared to the Na^+ charge site. Note that the bidentate M1[N,CO] structure is no longer among the low-energy structures once four waters are available for solvation of Na^+Gly.

4. Discussion

4.1. Trends in the experimental bond dissociation energies

Fig. 10 compares the hydration energies of Na^+ (obtained in previous CID work [6]) and Na^+Gly and the BDEs for loss of glycine [8]. For loss of glycine from $Na^+Gly(H_2O)_4$,

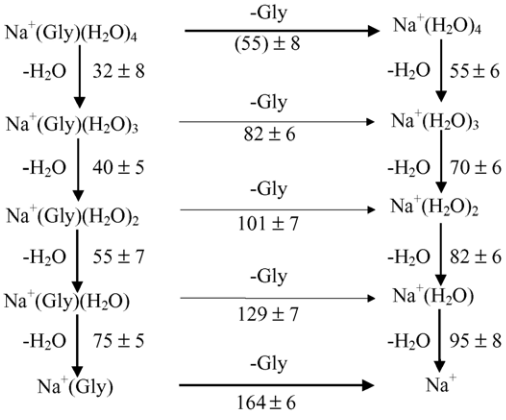

Fig. 10. Sequential hydration energies (kJ/mol) at 0 K of Na^+ and Na^+(Gly). $D_0(Na^+–Gly)$ is taken from reference [8]. $D_0[(H_2O)_xNa^+–H_2O]$ values are from reference [6].

we calculate an average value of 55 ± 8 kJ/mol from four different thermodynamic cycles, $D_0[Na^+(H_2O)_4–Gly] = D_0[Na^+Gly(H_2O)_{4-y} - yH_2O] + D_0[Na^+(H_2O)_{4-y} - Gly] - D_0[Na^+(H_2O)_{4-y} - yH_2O]$, where $y = 1–4$.

The reliability of the BDEs measured here can be tested by examining the consistency of the many thermodynamic cycles contained in Fig. 10. For instance, the sums of BDEs of the dissociation of $Na^+Gly(H_2O)_4$ via two different pathways (loss of glycine from $Na^+Gly(H_2O)_4$ followed by sequential loss of water molecules from $Na^+(H_2O)_4$ versus sequential loss of water molecules from $Na^+Gly(H_2O)_4$ followed by loss of glycine from Na^+Gly are 357 ± 15 and 366 ± 14 kJ/mol, respectively, where the deviation between the two sums is 9 ± 21 kJ/mol. Other cycles can be evaluated by examining the deviations in the bond energy sums for loss of glycine and then water versus loss of water and then glycine from the four $Na^+Gly(H_2O)_x$ complexes, $x = 1–4$. These deviations are 15 ± 12, 1 ± 14, 11 ± 12, and 4 ± 15 kJ/mol, respectively. In all cases, these comparisons confirm that the BDEs obtained in the present study are self-consistent and compatible with previous work in our lab [6,8].

Similar to the $Na^+(H_2O)_x$ system [6], the BDEs of water to sodiated glycine gradually decrease (from 75 ± 5 to 32 ± 8 kJ/mol) with increasing number of water molecules because of increasing steric interactions and decreasing effective charge on the sodium ion. In addition, experimental BDEs of glycine to $Na^+(H_2O)_x$ also decrease (from 164 ± 6 to 55 ± 8 kJ/mol) with increasing solvation. It is interesting to note that the BDEs of the first and second water to sodiated glycine (75 ± 5 and 55 ± 7 kJ/mol) are very close to those of the third and fourth water (70 ± 6 and 55 ± 6 kJ/mol) in the $Na^+(H_2O)_x$ system [6]. This correspondence implies that the solvation effect of glycine on a sodium ion nearly equals that of two water molecules, consistent with the bidentate structure for M1[N,CO]. Williams and coworkers obtained similar results for hydration of the Li^+Val complex. They determined that the BDEs for losing a water from $Li^+Val(H_2O)_x$, $x = 1–2$, using BIRD are 85 ± 3 and 60 ± 3 kJ/mol, respectively [15], which are slightly weaker than those of the third and fourth water (94 ± 4 and 71 ± 5 kJ/mol) in the $Li^+(H_2O)_x$ system [28].

The experimental binding energy of the fourth water to Na^+Gly is determined to be 32 ± 8 kJ/mol. This is higher than the energy associated with the hydrogen bonding in water, 23 kJ/mol [51]. This result implies that the fourth water is still binding to Na^+ or to glycine instead of hydrogen bonding to other water molecules. This conclusion is consistent with any of the low-lying structures of Fig. 9.

4.2. Conversion from 0 to 298 K

Conversion from experimental 0 to 298 K bond enthalpies and free energies are determined using frequencies calculated at the B3LYP/6-31G** level under the rigid rotor/harmonic oscillator approximation. These ΔH_{298} and ΔG_{298} values along with the conversion factors and 0 K enthalpies are re-

Table 5
Enthalpies and free energies (kJ/mol) of H_2O and glycine binding energies for $Na^+Gly(H_2O)_x$ at 0 and 298 K

Complex	Ionic product	ΔH_0[a]	$\Delta H_{298} - \Delta H_0$[b]	ΔH_{298}	$T\,\Delta S_{298}$[b]	ΔG_{298}
Na^+Gly	Na^+	164.0 (6)	2.7 (1.1)	166.7 (5.1)	34.4 (3.2)	132.3 (6.0)
$Na^+Gly(H_2O)$	Na^+Gly	75.3 (5)	−0.2 (1.7)	75.1 (5.3)	28.4 (8.2)	46.7 (9.7)
	$Na^+(H_2O)$	129.0 (7)	−1.0 (2.0)	128.0 (7.3)	35.6 (9.6)	92.3 (12.0)
$Na^+Gly(H_2O)_2$	$Na^+Gly(H_2O)$	54.9 (7)	1.5 (2.3)	56.5 (7.4)	37.8 (7.9)	18.6 (10.8)
	$Na^+(H_2O)_2$	100.9 (7)	0.4 (2.4)	101.2 (7.4)	45.9 (9.4)	55.3 (12.0)
$Na^+Gly(H_2O)_3$	$Na^+Gly(H_2O)_2$	40.0 (5)	−0.3 (3.6)	39.7 (6.2)	32.1 (11.8)	7.6 (13.3)
	$Na^+(H_2O)_3$	81.9 (6)	−0.5 (2.7)	81.4 (6.6)	45.5 (10.8)	35.9 (12.6)
$Na^+Gly(H_2O)_4$	$Na^+Gly(H_2O)_3$	32.4 (8)	3.2 (2.9)	35.6 (8.5)	44.8 (7.4)	−9.3 (11.3)
	$Na^+(H_2O)_4$	55.0 (8)	2.9 (2.4)	57.9 (8.3)	59.5 (7.6)	−1.6 (11.3)

Uncertainties in parentheses.
[a] Experimental values from this work and ref. [8] (Table 1).
[b] Values were computed using standard formulas and molecular constants calculated at the B3LYP/6-31G** level. The uncertainties correspond to 10% variations in the vibrational frequencies of the ligands and two-fold variations in the metal–ligand frequencies.

ported in Table 5. The uncertainties listed are determined by scaling most vibrational frequencies by ±10% and two-fold variations in the metal–ligand frequencies.

In general, room temperature reaction enthalpies, ΔH_{298}, are nearly the same as the 0 K values, ΔH_0, with the maximum difference of 3 kJ/mol in case of $x = 0$ and 4. The ΔG_{298} values decrease from 132.3 ± 6.0 to -1.6 ± 11.3 kJ/mol for losing glycine and from 46.7 ± 9.7 to -9.3 ± 11.3 kJ/mol for losing water. Note that the 298 K free energies for $Na^+Gly(H_2O)_4$ indicate that the equilibrium for generating these ions lies to the smaller $Na^+Gly(H_2O)_3$ complex. This is consistent with the low absolute intensities found for the $Na^+Gly(H_2O)_4$ ion beams.

We also examined the 298 K free energies of alternate conformers by including theoretical excitation energies (specifically those calculated at the MP2(full)//B3LYP level). In these calculations, both enthalpy and entropy corrections were calculated specifically for each conformer. In most cases, the conformer having the lowest enthalpy remains the ground state in terms of free energy. The only exception is for the case of $Na^+Gly(H_2O)_2$ where the 2W[bOH]-M6[CO] and 2W-M1[N,CO] conformers have free energies within 0.1 kJ/mol of one another, suggesting that an equilibrium distribution of these species would have nearly equal amounts of these two structures. Table 2 indicates that the 2W[bOH]-M6[CO] structure is favored if the excitation energies calculated using the density functional methods are used instead of the MP2 values.

4.3. Comparison of theoretical and experimental bond dissociation energies

As seen in Fig. 5, the BDEs obtained in our experiments and calculations for losing one water or glycine from a $Na^+Gly(H_2O)_x$ complex decrease monotonically with the BDEs for loss of glycine declining more rapidly than those for water loss. The monotonic decrease of BDEs for $Na^+Gly(H_2O)_x$ with increasing x is primarily a result of the increased charge solvation and increasing ligand–ligand repulsion. As each ligand donates electron density to the charged center at the metal, the effective charge is reduced, leading to weaker ion dipole and ion-induced dipole interactions. Further, in the proximity of the metal ion, the dipoles and induced dipoles on the ligands, which are aligned towards the metal ion, interact repulsively with one another, with the repulsion increasing with steric crowding in the complex.

Overall, the BDEs for losing one water from the ground state $Na^+Gly(H_2O)_x$ complexes calculated at four different levels show good agreement with the experimental values as shown in Fig. 5 and Table 4. The mean absolute deviations (MADs) between experiment and theory range from 3.2 to 5.8 kJ/mol, comparable to the average experimental uncertainty of ∼6 kJ/mol. The calculated BDEs for losing glycine from Na^+Gly show good agreement with the experimental value [8] at the B3LYP/6-311 + G(2d,2p)//B3LYP/6-31G* and B3P86/6-311 + G(2d,2p)//B3P86/6-31G* levels but the MP2(full)/6-311 + G(2d,2p)//B3LYP/6-31G** and MP2(full)/6-311 + G(2d,2p)//MP2(full)/6-31G** calculations yield results that are ∼12 kJ/mol lower. In contrast, the calculated BDEs for losing glycine from $Na^+Gly(H_2O)$ show good agreement with the experimental value at the MP2(full) level but are ∼10 and 16 kJ/mol higher than the experimental value at the B3P86 and B3LYP levels, respectively. The calculated BDEs for losing glycine from $Na^+Gly(H_2O)_x$, $x = 2$–4, calculated at four different levels are systematically higher than the experimental values by 9–22 kJ/mol. The MADs between experiment and theory for losing glycine, 9–14 kJ/mol (Table 4), exceed the average experimental error for all four levels of theory. The best agreement is achieved by the MP2(full)//MP2(full) calculations, whereas the B3P86//B3LYP calculations give the poorest agreement for loss of both glycine and water.

One possible explanation for these discrepancies is that the experiments are not measuring the same bond energies as those calculated. The comparison above is for the adiabatic bond energies, i.e., those for dissociation of the ground state complex to ground state products. If excited conformers are formed preferentially in the flow tube source under

our experimental conditions, then the experimental bond energies should be compared with different calculated values than these adiabatic bond energies. Hoyau and Ohanessian [49] have calculated a large, ∼80 kJ/mol, barrier for conversion between [N,CO] and [CO,OH] coordinated structures in Na^+Gly. It seems likely that water coordination would not substantially lower such a barrier in part because the water ligands would also need to be displaced as the glycine ligand is reoriented. Thus, once one of these structures is formed and stabilized, it is possible that it will not readily rearrange to alternate structures.

In our previous work, we concluded that the M1[N,CO] structure dominated the Na^+Gly complexes formed in our apparatus (>85%) [8]. Because the Na^+Gly_{x-1}–H_2O BDE does not exceed the putative 80 kJ/mol barrier, addition of a single water molecule to form $Na^+Gly(H_2O)$ should yield the 1W-M1[N,CO] ground state, predicted to be favored over M3[CO,OH] or M6[CO] coordination geometries by 5–8 kJ/mol (Table 2) (except at the B3P86 level). Therefore, it seems probable that the dc discharge flow tube source is producing primarily the 1W-M1[N,CO] conformer, which would then dissociate to form the ground state of Na^+Gly or $Na^+(H_2O)$ upon collision with Xe. This hypothesis is consistent with the good agreement between experimental and calculated BDEs for losing one water molecule or glycine from $Na^+Gly(H_2O)$, Fig. 5 and Table 4.

For $Na^+Gly(H_2O)_2$, calculations show that the addition of the second water molecule converts the preferred binding site from [N,CO] coordination of glycine to C=O coordination. The resulting adiabatic BDE for losing glycine is 10–19 kJ/mol higher than our experimental value. If the barrier for conversion between [N,CO] and [CO,OH] coordinated structures remains large (as for Na^+Gly), addition of H_2O to the ground state 1W-M1[N,CO] conformer has insufficient energy (55 kJ/mol) to anneal the two-water complex into its ground state. Therefore, we might generate primarily the 2W-M1[N,CO] conformer instead of the ground 2W[bOH]-M6[CO] conformer in the flow tube (and as noted above, the relative ΔG_{298} values of these two conformers suggests 2W-M1[N,CO] could be formed in abundance as well). The calculated BDEs for losing water or glycine from 2W-M1[N,CO] agree better with our experimental values as shown in Fig. 5. If similar considerations hold in the case of $Na^+Gly(H_2O)_3$, we might also produce the excited 3W-M1[N,CO] conformer in the flow tube source. Upon collisional excitation adequate to lose H_2O (40 kJ/mol), there is again too little energy to overcome an appreciable barrier for rearrangement to CO coordination, hence dissociation should occur diabatically to yield the 2W-M1[N,CO] complex. These diabatic bond energies are shown in Table 4 and Fig. 5 and can be seen to agree with experiment better than the adiabatic bond energies. However, in this case, it also seems feasible that the low-lying 3W[bN]-M9[CO] structure could be formed without a substantial barrier by addition of water to 2W-M1[N,CO]. If the 3W[bN]-M9[CO] structure dissociates to 2W-M1[N,CO], then the bond energies return to values within 2 kJ/mol of the adiabatic BDEs, because the excitation energies of the species are comparable (Table 2). For $Na^+Gly(H_2O)_4$, there is no low-lying M1[N,CO] structure, hence the 4W[bN]-M9[CO] structure is the likely species formed by addition of water to $Na^+Gly(H_2O)_3$ if no structural rearrangement is allowed. If this species dissociates to the 3W[bN]-M9[CO] complex, then the diabatic BDEs shown in Table 4 and Fig. 5 are obtained. These agree better with the experimental results than the adiabatic BDEs, such that the B3LYP and MP2//B3LYP values are within experimental error. Overall, a comparison of the experimental results with these diabatic bond energies yields MADs of 2 ± 1, 4 ± 3, 3 ± 2, and 3 ± 2 kJ/mol for loss of water calculated at the B3LYP, B3P86, MP2(full)//B3LYP, and MP2(full)//MP2(full) levels of theory, respectively, and of 7 ± 6, 7 ± 5, 6 ± 5, and 6 ± 5 kJ/mol for loss of glycine, respectively. Note that the former MADs are slightly better than those for the adiabatic BDEs (Table 4) and the latter are considerably better. Given the uncertainties in both the experimental and theoretical values, no definitive conclusions can be reached, although these comparisons do suggest that the conformers formed preferentially in the flow tube may be those favored kinetically, i.e., the M1-like structures characteristic of the Na^+Gly ground state.

4.4. Zwitterions

The evolution of the energetics of the zwitterionic form of the sodiated glycine complexes is interesting. For Na^+Gly, the zwitterion lies about 6–10 kJ/mol higher in energy than the M1[N,CO] ground state, with the M3[CO,OH] structure, the charge-solvated analog of the zwitterion, being nearly isoenergetic (−1 to 2 kJ/mol higher) [8]. Addition of a single water molecule stabilizes the neutral 1W-M3[CO,OH] structure, which now lies 0–6 kJ/mol higher than the 1W-M1[N,CO] ground state structure, and destabilizes the zwitterion, which lies 6–14 kJ/mol higher than the ground state (Table 2). A second water brings the 2W-M3[CO,OH] structure within 0–4 kJ/mol of the 2W-M1[N,CO] structure, while the structure incorporating a bridging water, 2W[bOH]-M6[CO], becomes the ground state. The lowest energy zwitterion also includes such a bridging water, such that this species lies −1 to 7 kJ/mol higher than 2W-M1[N,CO]. This water bridge is retained in the most stable zwitterionic structures as additional waters are included in the complex. Addition of a third water preferentially solvates the NH_3^+ charge site by 4–8 kJ/mol compared to the zwitterionic structure where all waters interact with Na^+, 3W[bO^-]-ZW[CO]. Addition of a fourth water continues to prefer solvating the NH_3^+ charge center, such that the 4W[2NH,bO^-]-ZW[CO] species is predicted to be the ground structure by B3P86 and only 1–8 kJ/mol higher than the nonzwitterionic ground conformation by the other three computational methods. If the fourth water solvates the sodium ion instead, the resultant zwitterion 4W[bCO,bO^-]-ZW[CO] is destabilized and lies 9–18 kJ/mol higher in energy than 4W[2NH,bO^-]-ZW[CO]. Given the low excitation en-

ergy of this latter conformer in the four water complex, it seems plausible that five or six waters should be sufficient to make the zwitterion the ground state conformer. Williams and coworkers reached a similar conclusion for hydration of the Na^+Val complex [13]. Not surprisingly, the present characterization of the structures upon sequential hydration indicates that the stability of the zwitterionic form of amino acids in solution is a consequence of being able to solvate all charge centers.

4.5. Structures of the complexes

High energy CID is often viewed as a viable means of obtaining structural information by assuming that bonding connectivities do not change upon dissociation. Of course, rearrangements are always possible, especially at lower energies where the energized species can have a longer lifetime. In the present studies, it is interesting to find that both $Na^+Gly(H_2O)_2$ and $Na^+Gly(H_2O)_3$ are observed to dissociate by loss of glycine at elevated energies, a process that competes with the much lower energy loss of a water molecule. These observations are suggestive that these two complexes have structures in which the water molecules are attached directly to the sodium ion. This is the case for all structures plausibly assigned above to the experimentally studied complexes on the basis of a comparison with theory: 2W[bOH]-M6[CO] and 2W-M1[N,CO] for $Na^+Gly(H_2O)_2$, and 3W[bOH]-M6[CO] and 3W[bN]-M9[CO] for $Na^+Gly(H_2O)_3$. In the case of the four water complex, there are several possible low energy structures according to calculations, and all of them have all four water molecules bonded close to Na^+ except for 4W[2NH,bO$^-$]-ZW[CO] and 4W[NH,bO$^-$]-ZW[CO]. If either of these structures is highly populated, this could explain why we fail to observe $Na^+(H_2O)_4$ as a product, although such a conclusion is not definitive because our sensitivity in this particular experiment is low.

Consideration of such structures also may provide a qualitative explanation of why the loss of the glycine ligand is less probable than expected on the basis of statistical considerations, i.e., the $\sigma_{0,j}$ values of Table 1 are smaller for glycine loss compared to water loss for $x = 1$ and 2 but not 3. Consider first the 1W-M1[N,CO] complex, in which the glycine is bound to Na^+ bidentate through the amide nitrogen and carbonyl, whereas the water is a monodentate ligand. It seems feasible that the smaller $\sigma_{0,j}$ for loss of glycine reflects a more convoluted dissociation path necessary to break both of the dative bonds, which could alternatively be modeled using a tighter transition state. For $Na^+Gly(H_2O)_2$, similar considerations would hold for dissociation of the 2W-M1[N,CO] complex (the diabatic dissociation discussed above), again explaining the different $\sigma_{0,j}$ values for glycine and water loss. However, the adiabatic dissociation pathway from 2W[bOH]-M6[CO], which binds the glycine ligand in a monodentate fashion, would be anticipated to be more facile, in contrast to the modeling parameters. Perhaps this provides additional evidence that the diabatic pathway is operative in these experiments. For $Na^+Gly(H_2O)_3$, both the 3W[bOH]-M6[CO] and 3W[bN]-M9[CO] structures postulated above have glycine bound to Na^+ as a monodentate ligand, consistent with statistical factors controlling the relative magnitudes of the competition between loss of this ligand and that of water. Additional evidence for the diabatic pathways may lie in the entropies of activation, $\Delta S^{\ddagger}_{1000}$, which increase smoothly for the diabatic pathways (Table 1), but not the adiabatic pathways.

5. Conclusions

The kinetic energy dependences of the collision-induced dissociation (CID) of $Na^+Gly(H_2O)_x$, where $x = 1$–4, are examined in a guided ion beam tandem mass spectrometer. The primary cross section in all cases is the loss of water from the complex. Sequential loss of water is also found for $x = 2$–4. Cross sections for losing glycine from the complexes $x = 1$–3 are also observed at much higher energies, with much smaller probabilities than for losing water. Zero Kelvin threshold energies for loss of water and glycine from the complexes are obtained by modeling the two cross sections of these competitive channels simultaneously using a competitive TCID model [19]. Experimental results show that the sequential binding energies for losing one water molecule and glycine from $Na^+Gly(H_2O)_x$ decrease monotonically with larger x. This trend can be attributed to the increasing ligand–ligand repulsion and decreasing effective charge on the sodium ion. Four different levels of ab initio calculations including zero point energy corrections for all and basis set superposition errors for MP2(full) calculations were performed for $Na^+Gly(H_2O)_x$, where $x = 0$–4. Within the experimental uncertainties, the calculated BDEs agree well with our experimental values, although somewhat better agreement is obtained if $Na^+Gly(H_2O)_x$ complexes are presumed to be kinetically trapped in low-energy conformers having M1[N,CO] coordination geometries.

All levels of theory predict similar structural changes as water molecules are added sequentially to Na^+Gly. In the absence of solvation, sodium ions bind in a bidentate configuration to the amino nitrogen and carbonyl oxygen of glycine, [N,CO] coordination, although this imposes energetic costs associated with deformation of the relatively rigid glycine backbone [8]. The first water attaches directly to sodium ion without further deforming the glycine backbone further. However, for $Na^+Gly(H_2O)_x$, where $x = 2$–4, the most favorable binding site for Na^+ changes from [N,CO] coordination to C=O coordination where one of the water molecules bridges to the hydroxyl group. Calculations show that all ground conformations of $Na^+Gly(H_2O)_x$, $x = 0$–3 are nonzwitterionic, whereas for $x = 4$, zwitterionic structures where both the Na^+ and NH_3^+ charge centers are solvated, 4W[2NH,bO$^-$]-ZW[CO] and 4W[NH,bO$^-$]-ZW[CO], are low-lying according to DFT but not MP2 calculations (Table 2). Somewhat counterintuitively, zwitterionic

structures corresponding to the ground state charge solvated conformations for $x = 2$–4 are destabilized by addition of water, because solvation of the Na^+ charge center alone reduces the ability of the complex to support the charge separation. However, for three or more water molecules, zwitterions in which the Na^+ and $NH_3{}^+$ charge centers are both solvated become the most stable zwitterionic structure. This species is believed to become the overall ground state as further hydration occurs, leading eventually to the expected solution phase zwitterion species.

Acknowledgments

This work is supported by the National Science Foundation under Grant No. CHE-0135517. A grant of computer time from the Center for High Performance Computing in University of Utah is gratefully acknowledged.

References

[1] C.H. Suelter, Science 168 (1970) 789.
[2] G.L. Prosise, J.Z. Wu, H. Luecke, J. Biol. Chem. 277 (2002) 50654.
[3] S.L. De Wall, E.S. Meadows, L.J. Barbour, G.W. Gokel, Proc. Natl. Acad. Sci. 97 (2000) 6271.
[4] M.M. Yamashita, L. Wesson, G. Eisenman, D. Eisenberg, Proc. Natl. Acad. Sci. 87 (1990) 5648.
[5] G. Bojesen, T. Breindahl, U.N. Andersen, Org. Mass Spectrom. 28 (1993) 1448.
[6] N.F. Dalleska, B.L. Tjelta, P.B. Armentrout, J. Phys. Chem. 98 (1994) 4191.
[7] J.S. Klassen, S.G. Anderson, A.T. Blades, P. Kebarle, J. Phys. Chem. 100 (1996) 14218.
[8] R.M. Moision, P.B. Armentrout, J. Phys. Chem. A 106 (2002) 10350.
[9] M.M. Kish, G. Ohanessian, C. Wesdemiotis, Int. J. Mass Spectrom. 227 (2003) 509.
[10] V. Ryzhov, R.C. Dunbar, B. Cerda, C. Wesdemiotis, J. Am. Soc. Mass Spectrom. 11 (2000) 1037.
[11] C. Ruan, M.T. Rodgers, J. Am. Chem. Soc. 126 (2004) 14600.
[12] R.M. Moision, P.B. Armentrout, Phys. Chem. Chem. Phys. 6 (2004) 2588.
[13] R.A. Jockusch, A.S. Lemoff, E.R. Williams, J. Phys. Chem. A 105 (2001) 10929.
[14] R.A. Jockusch, A.S. Lemoff, E.R. Williams, J. Am. Chem. Soc. 123 (2001) 12255.
[15] A.S. Lemoff, E.R. Williams, J. Am. Soc. Mass Spectrom. 15 (2004) 1014.
[16] H. Koizumi, P.B. Armentrout, J. Am. Soc. Mass Spectrom. 12 (2001) 480.
[17] H. Koizumi, X. Zhang, P.B. Armentrout, J. Phys. Chem. A 105 (2001) 2444.
[18] X.G. Zhang, P.B. Armentrout, Organometallics 20 (2001) 4266.
[19] M.T. Rodgers, P.B. Armentrout, J. Chem. Phys. 109 (1998) 1787.
[20] M.T. Rodgers, P.B. Armentrout, Mass Spectrom. Rev. 19 (2000) 215.
[21] M.T. Rodgers, P.B. Armentrout, J. Am. Chem. Soc. 122 (2000) 8548.
[22] M.T. Rodgers, K.M. Ervin, P.B. Armentrout, J. Chem. Phys. 106 (1997) 4499.
[23] K.M. Ervin, P.B. Armentrout, J. Chem. Phys. 83 (1985) 166.
[24] F. Muntean, P.B. Armentrout, J. Chem. Phys. 115 (2001) 1213.
[25] R.H. Schultz, K.C. Crellin, P.B. Armentrout, J. Am. Chem. Soc. 113 (1991) 8590.
[26] E.R. Fisher, P.B. Armentrout, J. Chem. Phys. 94 (1991) 1150.
[27] E.R. Fisher, B.L. Kickel, P.B. Armentrout, J. Chem. Phys. 97 (1992) 4859.
[28] M.T. Rodgers, P.B. Armentrout, J. Chem. Phys. A 101 (1997) 1238.
[29] E. Teloy, D. Gerlich, Chem. Phys. 4 (1974) 417.
[30] D. Gerlich, State-Selected and State-to-State Ion–Molecule Reaction Dynamics, Wiley, New York, 1992.
[31] N.F. Dalleska, K. Honma, L.S. Sunderlin, P.B. Armentrout, J. Am. Chem. Soc. 116 (1994) 3519.
[32] D.A. Hales, C.-X. Su, L. Li, P.B. Armentrout, J. Chem. Phys. 100 (1993) 1049.
[33] R.G. Gilbert, S.C. Smith, Theory of Unimolecular and Recombination Reactions, Blackwell Scientific Publications, Oxford, UK, 1990.
[34] P.J. Chantry, J. Chem. Phys. 55 (1971) 2746.
[35] E.V. Waage, B.S. Rabinovitch, Chem. Rev. 70 (1970) 377.
[36] D.A. Pearlman, D.A. Case, J.W. Caldwell, W.R. Ross, I. Cheatham, S. DeBolt, D. Ferguson, G. Seibel, P. Kollman, Comp. Phys. Commun. 91 (1995) 1.
[37] R.A. Kendall, E. Aprà, D.E. Bernholdt, E.J. Bylaska, M. Dupuis, G.I. Fann, R.J. Harrison, J. Ju, J.A. Nichols, J. Nieplocha, T.P. Straatsma, T.L. Windus, A.T. Wong, Comp. Phys. Comm. 128 (2000) 260.
[38] C.C.J. Roothan, Rev. Mod. Phys. 23 (1954) 69.
[39] J.S. Binkley, J.A. Pople, W.J. Hehre, J. Am. Chem. Soc. 102 (1951) 939.
[40] M.J. Frisch, G.W. Trucks, H.B. Schlegel, G.E. Scuseria, M.A. Robb, J.R. Cheeseman, V.G. Zakrzewski, J.A. Montgomery Jr., R.E. Stratmann, J.C. Burant, S. Dapprich, J.M. Millam, A.D. Daniels, K.N. Kudin, M.C. Strain, O. Farkas, J. Tomasi, V. Barone, M. Cossi, R. Cammi, B. Mennucci, C. Pomelli, C. Adamo, S. Clifford, J. Ochterski, G.A. Petersson, P.Y. Ayala, Q. Cui, K. Morokuma, P. Salvador, J.J. Dannenberg, D.K. Malick, A.D. Rabuck, K. Raghavachari, J.B. Foresman, J. Cioslowski, J.V. Ortiz, A.G. Baboul, B.B. Stefanov, G. Liu, A. Liashenko, P. Piskorz, I. Komaromi, R. Gomperts, R.L. Martin, D.J. Fox, T. Keith, M.A. Al-Laham, C.Y. Peng, A. Nanayakkara, M. Challacombe, P.M.W. Gill, B. Johnson, W. Chen, M.W. Wong, J.L. Andres, C. Gonzalez, M. Head-Gordon, E.S. Replogle, J.A. Pople, Gaussian 98, Revision A.11, Gaussian Inc., Pittsburgh, PA, 2001.
[41] A.D. Becke, J. Chem. Phys. 98 (1993) 5648.
[42] R. Ditchfield, W.J. Hehre, J.A. Pople, J. Chem. Phys. 54 (1971) 724.
[43] C. Möller, M.S. Plesset, Phys. Rev. 46 (1934) 618.
[44] A.D. McLean, G.S. Chandler, J. Chem. Phys. 72 (1980) 5639.
[45] J.B. Foresman, A.E. Frisch, Exploring Chemistry with Electronic Structure Methods, Gaussian Inc., Pittsburgh, PA, 1996.
[46] P.B. Armentrout, M.T. Rodgers, J. Phys. Chem. A 104 (2000) 2238.
[47] J.C. Amicangelo, P.B. Armentrout, Int. J. Mass Spectrom. 212 (2001) 301.
[48] F. Jensen, J. Am. Chem. Soc. 114 (1992) 9533.
[49] S. Hoyau, G. Ohanessian, Chem. Eur. J. 4 (1998) 1561.
[50] H. Ai, Y. Bu, J. Phys. Chem. B 108 (2004) 1241.
[51] S.J. Suresh, V.M. Naik, J. Chem. Phys. 113 (2000) 9727.